Wiley Analytical Science

Specific Heat Capacity Determination by DSC

April 19, 10:00am - 11:00am EDT

Specific heat capacity (cp) is an important, temperature-dependent material property and is often specified in material data sheets. It is a key property for improving technical processes such as injection molding, spray drying, or crystallization, as well as for the safety analysis of chemical processes and the design of chemical reactors.

Watch this session during the WAS Virtual Conference:

Dr. Jürgen Schawe

Register Now

This talk is sponsored by METTLER TOLEDO

Morphology of PU/PMMA Hybrid Particles from Miniemulsion Polymerization: Thermodynamic Considerations

CHIEN-YU LI,[1] WEN-YEN CHIU,[1,2,3] TRONG-MING DON[4]

[1]Department of Material Science and Engineering, National Taiwan University, Taipei, Taiwan, People's Republic of China

[2]Department of Chemical Engineering, National Taiwan University, Taipei, Taiwan, People's Republic of China

[3]Department of Polymer Science and Engineering, National Taiwan University, Taipei, Taiwan, People's Republic of China

[4]Department of Chemical and Materials Engineering, Tamkang University, Tamsui, Taipei County 25147, Taiwan, People's Republic of China

Received 21 October 2006; accepted 13 March 2007
DOI: 10.1002/pola.22086
Published online in Wiley InterScience (www.interscience.wiley.com).

ABSTRACT: The morphology of PU/PMMA hybrid particles prepared by miniemulsion polymerization was predicted through the consideration of their Gibbs free energy changes. Five morphological states of PU/PMMA hybrid particles were proposed and their Gibbs free energy changes were calculated. Before the formation of hybrid particles, the initial state included a monomer mixture of PU prepolymer, MMA, a chain extender, TMP, and an initiator, which was in droplets suspended in water containing SDS. Two assumptions were made. First, the densities of all states were the same. Secondly, secondary nucleation of particles was negligible. Thus the size of initial droplet and final particle was unchanged through miniemulsion polymerization. The interfacial tensions were measured by a pendant drop method and were used for calculation. The preferred morphology of PU/PMMA hybrid particle had the minimum value of ΔG_{phase}. Different NCO/OH ratios of PU and initiators of MMA were used to study the morphological change of PU/PMMA hybrid particles. When BD was used as the chain extender of PU, the hybrid particles showed the PU-rich phase as the shell and PMMA-rich as the core. When incorporating bisphenol A into PU polymer, the homogeneous structure of hybrid particle was preferred. © 2007 Wiley Periodicals, Inc. J Polym Sci Part A: Polym Chem 45: 3359–3369, 2007
Keywords: morphology; polyurethanes; thermodynamics

INTRODUCTION

To achieve better mechanical properties and higher colloid stability, a hybrid polymer particle containing two polymers is generally prepared as designed.[1–3] In recent years, miniemulsion polymerization is a new way to prepare the hybrid particle. There are some documents of preparing core-shell latex through miniemulsion polymerization.[4–7] However, the morphological changes of the hybrid particles with experimental variables, such as compositions of

Correspondence to: W.-Y. Chiu (E-mail: ycchiu@ccms.ntu.edu.tw)

Journal of Polymer Science: Part A: Polymer Chemistry, Vol. 45, 3359–3369 (2007)

monomers, types of initiators, and other polymerization conditions, were not fully understood.

Most polymer blends contain thermodynamically immiscible components. Their morphology usually has a larger influence on mechanical properties. It is well known that the morphology of polymer blends is influenced by the blend composition, preparation conditions, and interfacial tension between two polymers. Latex system with well-designed particle morphology is useful to manufacture advanced engineering plastics with high tensile strength, improved toughness, and other high-added values. Composite latex particles of different morphologies are usually prepared by seeded emulsion polymerization techniques where a second monomer is synthesized in the presence of seed latex particles. Investigation of the morphology of core-shell latex and the factors controlling it are the goal of many papers published in previous years. Most researched systems in the literatures are PS/PMMA[8–10] and PS/PBA.[11,12] In these earlier documents, the controlling factors fall into two broad categories: thermodynamics and kinetics. Thermodynamic factors determine the equilibrium morphology of final particles, whereas kinetic ones determine the ease of such thermodynamically favored morphology.

In the aspects of thermodynamics, Torza and Mason[13] first showed the interfacial behavior of systems including three immiscible liquids. They examined the required states for a liquid to engulf an initial droplet when both were immersed in a continuous phase. Their analysis showed that the interfacial tension was one of the main factors controlling the morphology of particles. Dimonie et al.[14] also reported the viscosity of the polymerization locus, which related to the chain mobility influenced morphology as well. The following work from Chen et al.[15] demonstrated an important mathematical model combining the study of Sundberg et al.[16] to describe the free energy changes corresponding to PS/PMMA latex morphology. This model combining the analysis of interfacial tension predicted the latex morphology successfully.

In addition, methods to measure interfacial tension between immiscible fluid phases have been developed for many years. For instance, Van der Waals acid–base approach,[17] the soap titration,[11] drop-weight volume,[18] and pendant drop[19–21] could be used to determine interfacial tensions. Other methods have been reviewed in detail by Rusanov and Prokhorov.[22] In our work, the pendant drop was used to measure the interfacial tension. This method has the following advantages: it is a simple-mathematical analysis; results are independent of the contact angle between the fluid interface and the apparatus; photographs of drop-shape can be analyzed instantaneously; it is a static method and therefore would not be influenced by viscosity; only small samples are needed and high accuracy results can be obtained.

By thermodynamic consideration, the Gibbs free energy changes of PU/PMMA hybrid particles prepared from miniemulsion polymerization were calculated and related to the morphology.

THERMODYNAMIC CONSIDERATIONS OF THE PARTICLE MORPHOLOGY

By considering the following assumptions for morphology development in miniemulsion polymerization, the change of Gibbs free energy was regarded as the driving force. As shown in Figure 1, the initial state included a monomer mixture of PU prepolymer, MMA, a chain extender, TMP, and an initiator, which was in droplets suspended in water containing SDS. Five possible states of final particles were considered in this study. The total Gibbs free energy change can be expressed as

$$\Delta G_{\text{total}} = \Delta G_{\text{poly}} + \Delta G_{\text{phase}}$$

ΔG_{poly}: from the polymerization; ΔG_{phase}: from the change of morphology and interfacial tension.

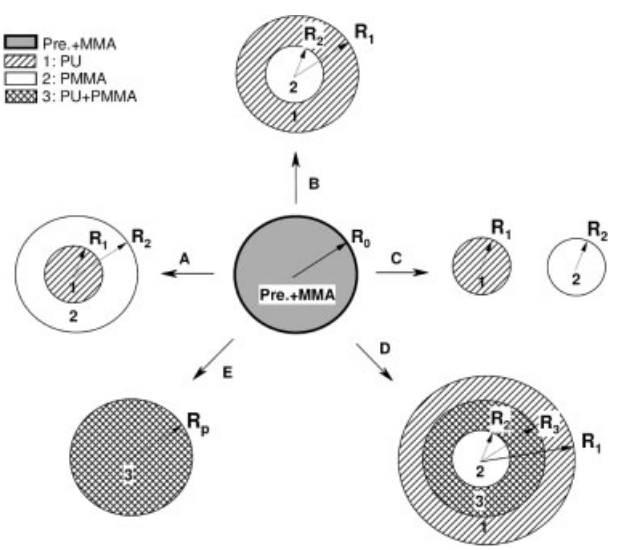

Figure 1. Morphological states of PU/PMMA hybrid particles.

Because polymerization occurred, $\Delta G_{poly} < 0$. If the final state could be formed, ΔG_{total} should be negative. Hence, the value of ΔG_{phase} would determine the morphology of the final state. In this work, we thus focused on the Gibbs free energy change (ΔG_{phase}) from the change of morphology and interfacial tension.

Equations for ΔG_{phase}

From thermodynamic equation, the internal energy U at constant temperature is

$$dU = T\,dS + dW$$

where T is temperature, S is entropy, and W is work done by the system.

The change of morphology of particles from initial to final state creates new interfaces. If the surface tension γ is a real force acting along the surface, it will produce the work $\gamma\,dA$, where A is the surface area. Then we get

$$dW = \gamma\,dA - d(PV)$$

$$dU = T\,dS + \gamma\,dA - d(PV)$$

The integrating form at constant pressure is

$$U = TS + \gamma A - PV$$

Hence, the Gibbs free energy is

$$\begin{aligned} G_{phase} &= H - TS \\ &= U + PV - TS \\ &= \gamma A \end{aligned}$$

And the total Gibbs free energy change can Be expressed as

$$\Delta G_{phase} = \Delta(\gamma A)$$

or

$$\Delta G_{phase} = \sum \gamma_{ij} A_{ij} - \gamma_{mw} A_{mw} \qquad (1)$$

where γ_{ij} is the interfacial tension between i and j and A_{ij} is the corresponding interfacial area. γ_{mw} is the interfacial tension of initial monomer droplet suspended in water and A_{mw} is its interfacial area. Each of the final states, A–E in Figure 1, had different total Gibbs free energy change due to its different morphology. The thermodynamically preferred morphology of a system will be the one that had minimum value of ΔG_{phase}. If all γ_{ij} can be measured, the Gibbs free energy change can be calculated. Thus, the prediction of preferred morphology resulted in a practical application. Two important assumptions were made as: (1) the densities of all states were the same; (2) secondary nucleation of particles was negligible. Thus the size of initial droplet and final particle was unchanged through miniemulsion polymerization. Following was the description of Gibbs free energy change per unit area for five final states.

State A: PU as the Core and PMMA as the Shell

The Gibbs free energy change for state A was

$$\begin{aligned} \Delta G_a &= \gamma_{12} A_{12} + \gamma_{2w} A_{2w} - \gamma_{mw} A_{mw} \\ &= \gamma_{12} 4\pi R_1^2 + \gamma_{2w} 4\pi R_2^2 - \gamma_{mw} 4\pi R_0^2 \end{aligned} \qquad (2)$$

where γ_{12}, γ_{2w}, and γ_{mw} were the interfacial tensions between the phases of PU/PMMA, PMMA/water and monomers/water, respectively. R_1, R_2, and R_0 were the radius of PU core, final particle, and initial droplet, respectively. To describe the free energy change per unit surface area of initial droplet, eq 2 could be rearranged as

$$\Delta\psi_a = \frac{\Delta G_a}{4\pi R_0^2} = \gamma_{12}\left(\frac{R_1}{R_0}\right)^2 + \gamma_{2w}\left(\frac{R_2}{R_0}\right)^2 - \gamma_{mw} \qquad (3)$$

where $\Delta\Psi_a$ was the free energy change per unit area of particle.

To define the volume fraction of PMMA in the final particle, ϕ_2 as

$$\begin{aligned} \phi_2 = \frac{V_2}{V_t} = \frac{\frac{4}{3}\pi R_2^3 - \frac{4}{3}\pi R_1^3}{\frac{4}{3}\pi R_2^3} = \frac{R_2^3 - R_1^3}{R_2^3} = 1 - \left(\frac{R_1}{R_2}\right)^3 \\ => \frac{R_1}{R_2} = (1-\phi_2)^{1/3} \end{aligned} \qquad (4)$$

By Using $R_2 = R_0$ (for ideal miniemulsion) and ϕ_2, eq 3 turned into

$$\Delta\psi_a = \gamma_{12}(1-\phi_2)^{2/3} + \gamma_{2w} - \gamma_{mw} \qquad (5)$$

State B: PMMA as the Core and PU as the Shell

Similar analysis was applied to state B as follows:

$$\phi_2 = \frac{V_2}{V_t} = \frac{\frac{4}{3}\pi R_2^3}{\frac{4}{3}\pi R_1^3} = \frac{R_2^3}{R_1^3} = \left(\frac{R_2}{R_1}\right)^3$$
$$=> \frac{R_2}{R_1} = \phi_2^{1/3} = \frac{R_2}{R_0}$$

$$\Delta G_b = \gamma_{12}A_{12} + \gamma_{1w}A_{1w} - \gamma_{mw}A_{mw}$$
$$= \gamma_{12}4\pi R_2^2 + \gamma_{1w}4\pi R_1^2 - \gamma_{mw}4\pi R_0^2$$

and

$$\Delta\psi_b = \frac{\Delta G_b}{4\pi R_0^2} = \gamma_{12}\left(\frac{R_2}{R_0}\right)^2 + \gamma_{1w}\left(\frac{R_1}{R_0}\right)^2 - \gamma_{mw}$$
$$= \gamma_{12}\phi_2^{2/3} + \gamma_{1w} - \gamma_{mw} \quad (6)$$

State C: Individual Particles of PMMA and PU

The volume fraction of PMMA was as

$$\phi_2 = \frac{V_2}{V_t} = \frac{\frac{4}{3}\pi R_2^3}{\frac{4}{3}\pi R_1^3 + \frac{4}{3}\pi R_2^3} = \frac{R_2^3}{R_1^3 + R_2^3} = \frac{1}{\left(\frac{R_1}{R_2}\right)^3 + 1}$$
$$=> \frac{R_1}{R_2} = \left(\frac{1}{\phi_2} - 1\right)^{1/3}$$

Here $R_0 \neq R_1 \neq R_2$, therefore

$$\phi_2 = \frac{V_2}{V_t} = \frac{R_2^3}{R_0^3}$$
$$=> \frac{R_2}{R_0} = \phi_2^{1/3}$$
$$=> \frac{R_1}{R_0} = (1 - \phi_2)^{1/3}$$

The free energy change was expressed as

$$\Delta G_c = \gamma_{1w}A_{1w} + \gamma_{2w}A_{2w} - \gamma_{mw}A_{mw}$$
$$= \gamma_{1w}4\pi R_1^2 + \gamma_{2w}4\pi R_2^2 - \gamma_{mw}4\pi R_0^2$$

and

$$\Delta\psi_c = \frac{\Delta G_c}{4\pi R_0^2} = \gamma_{1w}\left(\frac{R_1}{R_0}\right)^2 + \gamma_{2w}\left(\frac{R_2}{R_0}\right)^2 - \gamma_{mw}$$
$$= \gamma_{1w}(1 - \phi_2)^{2/3} + \gamma_{2w}\phi_2^{2/3} - \gamma_{mw} \quad (7)$$

State D: PMMA as the Core, PU/PMMA as the Intermediate Layer, and PU as the Shell

First, we defined the weight fraction of PU (x) and volume fraction of PMMA (ϕ_2). Thus the relation of R_1, R_2, and R_3 was as

$$x = \frac{W_{PU}}{W_{PU} + W_{PMMA}}$$

$$\phi_2 = \frac{V_2}{V_t} = 1 - x$$
$$=> \frac{R_2^3 + \phi_{32}(R_3^3 - R_2^3)}{R_1^3} = 1 - x$$
$$=> \phi_{32}\left(\frac{R_3}{R_1}\right)^3 + \phi_{31}\left(\frac{R_2}{R_1}\right)^3 = 1 - x$$
$$=> \left(\frac{R_3}{R_1}\right)^3 = \frac{1-x}{\phi_{32}} - \frac{\phi_{31}}{\phi_{32}}\left(\frac{R_2}{R_1}\right)^3 \text{ or}$$
$$\left(\frac{R_2}{R_1}\right)^3 = \frac{1-x}{\phi_{31}} - \frac{\phi_{31}}{\phi_{31}}\left(\frac{R_3}{R_1}\right)^3$$

where ϕ_{31} and ϕ_{32} are the volume fractions of PU and PMMA in the intermediate layer, respectively.

As a result, the free energy change can be expressed in terms of R_2/R_0

$$\Delta G_d = \gamma_{23}A_{23} + \gamma_{13}A_{13} + \gamma_{1w}A_{1w} - \gamma_{mw}A_{mw}$$
$$= \gamma_{23}4\pi R_2^2 + \gamma_{13}4\pi R_3^2 + \gamma_{1w}4\pi R_1^2 - \gamma_{mw}4\pi R_0^2$$

and

$$\Delta\psi_d = \frac{\Delta G_d}{4\pi R_0^2} = \gamma_{23}\left(\frac{R_2}{R_0}\right)^2 + \gamma_{13}\left(\frac{R_3}{R_0}\right)^2 + \gamma_{1w}\left(\frac{R_1}{R_0}\right)^2 - \gamma_{mw}$$
$$= \gamma_{23}\left(\frac{R_2}{R_0}\right)^2 + \gamma_{13}\left(\frac{\phi_2}{\phi_{32}} - \frac{\phi_{31}}{\phi_{32}}\left(\frac{R_2}{R_0}\right)^3\right)^{2/3}$$
$$+ \gamma_{1w} - \gamma_{mw} \quad (8)$$

State E: Homogeneous PU/PMMA Particle

If there was no phase separation occurred through miniemulsion polymerization, the free energy change was expressed as

$$\Delta G_e = \gamma_{pw}A_{pw} - \gamma_{mw}A_{mw} = \gamma_{pw}4\pi R_p^2 - \gamma_{mw}4\pi R_0^2$$
$$\Delta\psi_e = \frac{\Delta G}{4\pi R_0^2} = \gamma_{pw}\left(\frac{R_p}{R_0}\right)^2 - \gamma_{mw} = \gamma_{pw} - \gamma_{mw} \quad (9)$$

Therefore, by measuring the interfacial tension, the free energy change could be calculated from eqs 5–9 for five final states of particles, respectively.

EXPERIMENTAL

Materials

Isophorone diisocyanates (IPDI; Lancaster), 1,4-butanediol (BD; TEDIA), bisphenol A (BisA; TCI), trimethylol propane (TMP; ACROS), dibutyltin dilaurate (SnDBL; TCI), sodium dodecyl sulfate (SDS; TCI), hexadecane (HD; TCI), benzoyl peroxide (BPO; ACROS), potassium persulfate(KPS; TCI), and hydroquinone (HQ; TCI) were used without further purification. Polypropylene glycol (PPG; Showa), with an average molecular weight of 1000 (g/mol), was dried under vacuum at 80 °C for 24 h before use. Methyl methacrylate (MMA; Showa) was distilled to remove impurities and then stored in refrigerator before use.

Synthesis of PU Prepolymer

The synthesis of PU prepolymer was carried out in a 100-mL round-bottom, three-necked flask with a magnetic stirrer, thermometer, condenser, nitrogen inlet, and an outlet. Reaction temperature was set at 60 °C and was controlled by immersion in an isothermal oil bath. IPDI (1.23 g) and PPG1000 (2.76 g) dissolved in MMA (1.6 g) were charged into the flask and then heated to the reaction temperature. Subsequently, SnDBL catalyst (0.1 wt % based on the total monomer weight) was added into the solution. The equivalent ratio of IPDI and PPG1000 was 2/1. The theoretical NCO value was determined using a standard dibutylamine back titration method. After achieving the theoretical NCO value, NCO-terminated prepolymers were cooled down to room temperature and then were stored in refrigerator before use.

Synthesis of PU Latex

An oil phase, NCO-terminated prepolymers (5.59 g), isophorone diisocyanates (0.86 g; if needed), hexadecane (4.4 wt %), 1,4-butanediol (0.125 g) or bisphenol A (0.315 g), dibutyltin dilaurate (0.1 wt %), and trimethylol propane (0.125 g) were stirred together. Sodium dodecyl sulfate (0.8 wt %) was dissolved in deionized water as a water phase. Then the oil and water phases were mixed and stirred for 10 min. Preemulsion was prepared by ultrasonifying the mixtures for 12 min. All the above steps were proceeded in an ice bath to prevent the premature polycondensation reaction. The miniemulsion was introduced to a 250-mL round-bottom, four-necked separable flask with a mechanical stirrer, thermometer, condenser, nitrogen inlet, and an outlet. Synthesis of PU latex was carried out at 70 °C for 3 h. To obtain the dried PU latex, samples were washed with water, filtered, and dried by lyophilization. Two different chain extenders were used to obtain PU polymers. The first one was BD chain extender with NCO/OH = 1.7, 1.0 (BD/1.7; BD/1.0) and the second one was BisA chain extender with NCO/OH = 1.0 (BisA/1.0).

Synthesis of PMMA Latex

Two kinds of initiators were used: BPO and KPS. In an oil phase, MMA (16.13 g), HD (4.4 wt %), and initiator (1 wt %) were stirred together. SDS (0.8 wt %) was dissolved in deionized water as a water phase. Then the oil and water phases were mixed and stirred. A miniemulsion was prepared by ultrasonifying the mixtures for 12 min. All the above steps were proceeded in an ice bath. The miniemulsion was introduced to a 250-mL round-bottom, four-necked separable flask with a mechanical stirrer, thermometer, condenser, nitrogen inlet, and an outlet. After 5 min, KPS (if needed) was added into reactor. Synthesis of PMMA latex was carried out at 70 °C for 3 h. To obtain the dried PMMA latex, samples were washed with water, filtered, and dried by lyophilization. Two different PMMA were synthesized, namely, PMMA-BPO from BPO initiator and PMMA-KPS from KPS initiator.

Synthesis of PU/PMMA Hybrid Latex

In an oil phase, NCO-terminated prepolymer (5.59 g), MMA (15.37 g), HD (4.4 wt %), BD (0.125 g), SnDBL (0.1 wt %), TMP (0.125 g), and BPO (1 wt %) were stirred together. SDS (0.8 wt %) was dissolved in deionized water as a water phase. Then the oil and water phases were mixed and stirred. A miniemulsion was prepared by ultrasonifying the mixtures for 12 min. All the above steps were proceeded in

an ice bath to prevent the premature polymerization reaction. The miniemulsion was introduced to a 250-mL round-bottom, four-necked separable flask with a mechanical stirrer, thermometer, condenser, nitrogen inlet, and an outlet. Synthesis of PU/PMMA polymer was carried out at 70 °C for 3 h.

Analysis

Contact Angle Measurements

PU and PMMA latex were poured into steel molds at 100 °C for 24 h and their films were obtained. Two liquids, water and ethylene glycol, were used as the probe liquids. A releasing probe liquid (0.05 mL) was dropped onto the surface of polymer film from a syringe. Contact angles of each drop (θ_w and θ_{EG}) were recorded by the instrument, Olympus, model SZ-ST. Three drops were taken to give the value in average. As shown in Table 1, there were five kinds of polymer films. Furthermore, from the transform Harmonic-mean equation,[23]

$$(1+\cos\theta_w)\gamma_w = 4\left(\frac{\gamma_w^d\gamma^d}{\gamma_w^d+\gamma^d}+\frac{\gamma_w^p\gamma^p}{\gamma_w^p+\gamma^p}\right)$$

$$(1+\cos\theta_{EG})\gamma_{EG} = 4\left(\frac{\gamma_{EG}^d\gamma^d}{\gamma_{EG}^d+\gamma^d}+\frac{\gamma_{EG}^p\gamma^p}{\gamma_{EG}^p+\gamma^p}\right)$$

Surface tension components of water: $\gamma_w^p = 50.7$ mN m^{-1}, $\gamma_w^d = 22.1$ mN m^{-1}, $\gamma_w = 72.8$ mN m^{-1}; Ethylene glycol (EG): $\gamma_{EG}^p = 17.6$ mN m^{-1}, $\gamma_{EG}^d = 30.1$ mN m^{-1}, $\gamma_{EG} = 47.7$ mN m^{-1} were based on the ref. 23. Then the polar component γ^p and the dispersive component γ^d of the surface tension of each polymer could be calculated.

Table 1. Contact Angles and Surface Tension Components of PU and PMMA Films

Polymer	Θ_w[a] (°)	Θ_{EG}[b] (°)	γ^p (mN m^{-1})	γ^d (mN m^{-1})
BD/1.7	78.6	40.7	12.6	24.9
BD/1.0	91.8	51.0	5.0	32.2
BisA/1.0	93.5	53.2	4.2	32.6
PMMA-BPO	85.3	44.1	8.2	29.5
PMMA-KPS	84.1	43.3	8.9	28.7

[a] Surface tension components of water: $\gamma_w^p = 50.7$ mN m^{-1}, $\gamma_w^d = 22.1$ mN m^{-1}, $\gamma_w = 72.8$ mN m^{-1}.
[b] Surface tension components of ethylene glycol (EG): $\gamma_{EG}^p = 17.6$ mN m^{-1}, $\gamma_{EG}^d = 30.1$ mN m^{-1}, $\gamma_{EG} = 47.7$ mN m^{-1}.

Interfacial Tension Measurements (γ_{1w}, γ_{2w}, γ_{mw}, γ_{12}, and γ_{pw})

The interfacial tension measurements were done by the pendent drop method through Sinterface Tensiometer, PAT-2 with CCD camera. Interfacial tensions between monomer phase and water/SDS/KPS (if needed) (γ_{mw}), PU and water/SDS (γ_{1w}), PMMA and water/SDS (γ_{2w}) were measured at 70 °C. For the measurement of γ_{mw}, the monomer phase included PU prepolymer, MMA, IPDI, BD or BisA, and TMP. A drop of monomer phase from a syringe was immersed into the water phase and γ_{mw} was calculated instantaneously by computer based on the shape of drop. Twelve weight ratios of monomer phases were tested. Similarly, for the measurement of γ_{1w}, PU polymer was dissolved previously into IPDI and PPG monomers. And then the drop of PU/IPDI/PPG was immersed into water/SDS/KPS (if needed) phase. By increasing the concentration of PU polymer, a constant value of γ was obtained and was regarded as γ_{1w}. In this work, there were four values of γ_{1w} (BD/BPO/1.7, BD/BPO1.0, BD/KPS/1.0, and BisA/KPS/1.0). For the measurement of γ_{2w}, PMMA polymer was dissolved into MMA monomer. The drop of PMMA/MMA was immersed into water/SDS/KPS (if needed) phase. By increasing the concentration of PMMA polymer, a constant value of γ was obtained and was regarded as γ_{2w}. In this work, there were two kinds of γ_{2w}, which were two types of PMMA polymers (PMMA-BPO, PMMA-KPS).

The interfacial tension between PU and PMMA (γ_{12}) was calculated based on the results in Table 1 and the Harmonic-mean equation,[23]

$$\gamma_{12} = \gamma_1 + \gamma_2 - 4\left(\frac{\gamma_1^d\gamma_2^d}{\gamma_1^d+\gamma_2^d}+\frac{\gamma_1^p\gamma_2^p}{\gamma_1^p+\gamma_2^p}\right)$$

γ_1: Surface tension of PU polymer; γ_2: Surface tension of PMMA polymer.

γ_1^d and γ_1^p were the dispersive and polar components of surface tension of PU polymer, respectively.

γ_2^d and γ_2^p were the dispersive and polar components of surface tension of PMMA polymer, respectively.

And γ_{pw} in eq 9 was estimated according to the mixing rule $(1-x)\gamma_{1w} + (x)\gamma_{2w}$; x = PMMA/(PMMA+PU) weight ratio. Table 2 summarized

Table 2. Interfacial tensions of monomer/water, PU/water, PMMA/water, and PU/PMMA

Polymer	PU/PMMA weight ratios[a]	γ_{mw} (10^{-3} N m^{-1})	γ_{1w}	γ_{2w}	γ_{12}[b]	γ_{pw}[c]
BD/1.7<->PMMA-BPO	20/80	4.6	2.9	4.9	1.3	4.50
	30/70	3.9				4.30
	40/60	3.4				4.10
BD/1.0<->PMMA-BPO	20/80	4.7	3.1	4.9	0.9	4.54
	30/70	4.0				4.36
	40/60	3.6				4.18
BD/1.0<->PMMA-KPS	20/80	3.4	2.9	3.5	1.3	4.42
	30/70	2.0				4.23
	40/60	1.4				4.04
BisA/1.0<->PMMA-KPS	20/80	3.3	2.9	3.5	1.9	3.38
	30/70	2.4				3.32
	40/60	1.8				3.26

[a] PU indicates the PU prepolymer, IPDI, TMP, and chain extenders.
[b] Based on Harmonic-mean equation.
[c] Based on $(1-x)\gamma_{1w} + (x)\gamma_{2w}$; x = PMMA/(PMMA+PU) weight ratio.

the data of interfacial tensions of different systems.

TEM Cross-Section Morphology

The morphology of particles of hybrid latex was characterized by TEM (JOEL JEM-1230 with Gatan DualVision CCD Camera). To observe the phase distribution in particles, the ultrathin cross section of the hybrid sample was stained by phosphotungstic acid (PTA) for 5 min. PTA can stain the PU phase but not the PMMA phase, so under the observation of TEM, the PU phase is dark, whereas the PMMA phase is bright.

RESULTS AND DISCUSSION

Contact Angles and Surface Tension Components of Polymer Films

Contact angles of five polymer films were shown in Table 1. For PU films, PU prepared with NCO/OH = 1.7 had the lowest value of contact angle, which meant the highest hydrophilic property. Due to the hydrophilic property of BD chain extender, PU with BD chain extender showed the lower contact angle than PU with Bisphenol A chain extender. Furthermore, by comparing contact angles of PMMA films, PMMA synthesized with KPS initiator was more hydrophilic than PMMA with BPO initiator because of the ion charge of KPS.

Interfacial Tensions of Monomer/Water, PU/Water, PMMA/Water, and PU/PMMA

The interfacial tensions of monomers/water (γ_{mw}) were shown in Table 2. It was apparently affected by different weight ratios of PU/PMMA. In the existence of NCO-terminated PU prepolymer, monomer phase would turn into more hydrophilic and γ_{mw} decreased. Hence, with increasing hydrophilic PU content, γ_{mw} decreased.

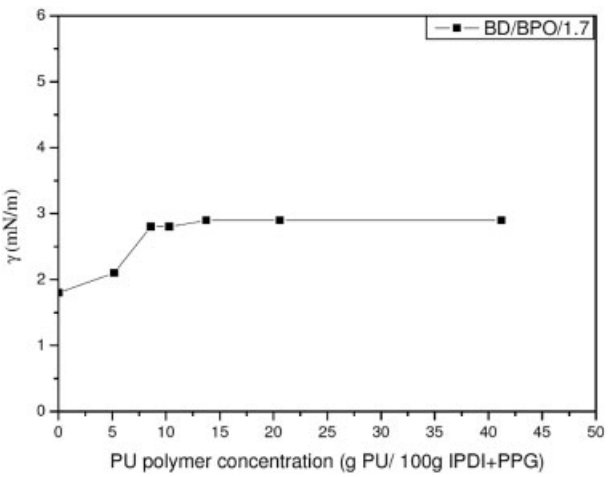

Figure 2. Interfacial tensions between PU+IPDI+PPG and water with different PU polymer concentrations for BD/BPO/1.7 system.

Besides, if excess IPDI was added (BD/1.7), it also resulted in a higher hydrophilic monomer phase and thus a lower γ_{mw} was obtained. To measure the interfacial tension of PU/water (γ_{1w}), PU polymer phase with different concentrations was dissolved previously into its monomers. As increasing PU polymer (BD/1.7) concentration, Figure 2 indicated the value of γ would increase in the beginning. It was because that PU polymer, which was hydrophobic than monomers, reduced the hydrophilic ability of monomer phase. As more PU polymer was added, γ approached a constant value at 2.9 mN m^{-1} and the value was regarded as the interfacial tension of PU(BD/1.7)/water (γ_{1w}). The same phenomenon was observed in the other PU polymer systems. Figure 3 revealed that the interfacial tension between PU polymer (BD/1.0) and water was 3.1 mN m^{-1}, which was higher than the value of PU polymer (BD/1.7). It could be seen that the higher amount of NCO groups indeed led to a higher hydrophilic monomer phase. Figures 4 and 5 showed the interfacial tension between PU polymer (BD/1.0) and water phase was 2.9 mN m^{-1}, as using BisA as the chain extender (BisA/1.0), γ was 2.9 mN m^{-1}.

Different initiators for MMA polymerization also influenced the interfacial tension. By using BPO as the initiator, as shown in Figure 6, the interfacial tension (γ_{2w}) between PMMA/MMA and water was 4.9 mN m^{-1}. However, when KPS was used as the initiator, Figure 7 showed that γ_{2w} reduced to 3.5 mN m^{-1}. PMMA prepared from KPS initiator had much lower value of γ_{2w} than PMMA synthesized by BPO initiator. It was ascribed to the ion charge of KPS that reducing the interfacial tension.

According to the Harmonic-mean equation, the interfacial tension (γ_{12}) of PU and PMMA was calculated by their contact angles. It could be seen that γ_{12} was much lower than the other interfacial tensions.

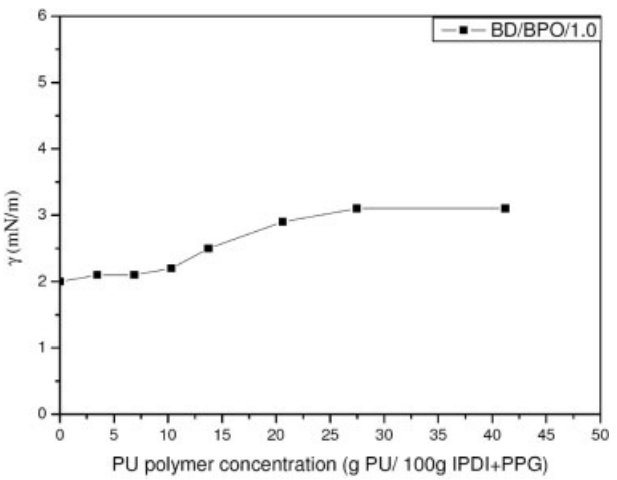

Figure 3. Interfacial tensions between PU+IPDI +PPG and water with different PU polymer concentrations for BD/BPO/1.0 system.

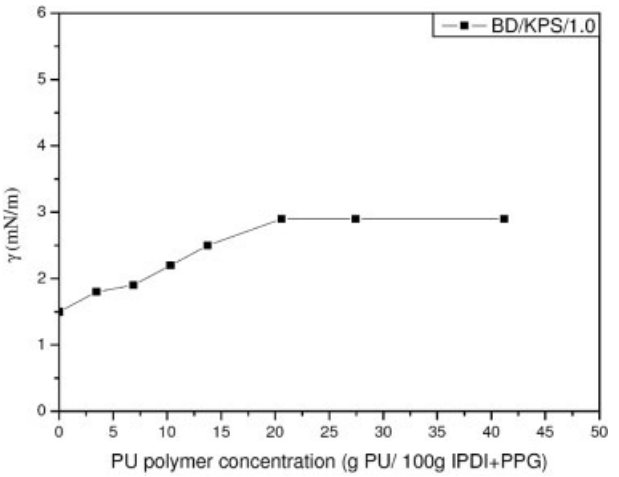

Figure 4. Interfacial tensions between PU+IPDI +PPG and water with different PU polymer concentrations for BD/KPS/1.0 system.

Consideration of Four PU/PMMA Systems

Based on interfacial tensions, the free energy changes of five final states with different PU/PMMA weight ratios could be calculated. The preferred morphology of PU/PMMA hybrid par-

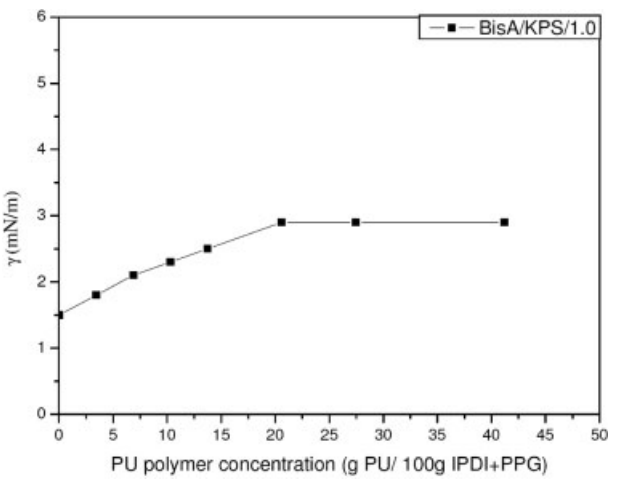

Figure 5. Interfacial tensions between PU+IPDI +PPG and water with different PU polymer concentrations for BisA/KPS/1.0 system.

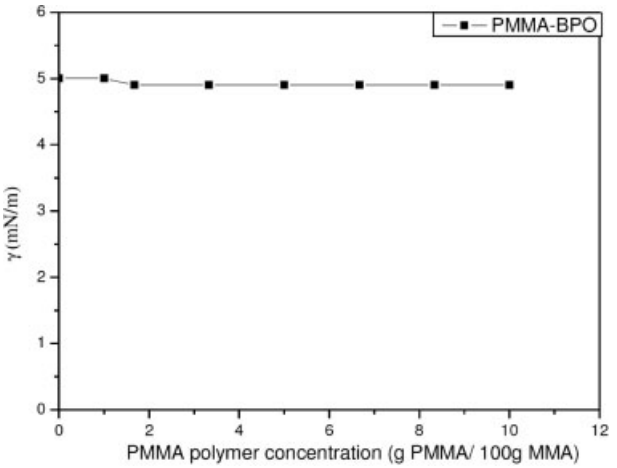

Figure 6. Interfacial tensions between PMMA-BPO/MMA and water with different PMMA polymer concentrations for PMMA-BPO system.

ticle had a minimum ΔG_{phase} value. As shown in Figure 8, BD/BPO system with NCO/OH = 1.7 had the order of free energy change A > C > E > B > D. The minimum ΔG_{phase} was the state D, which had the three-layer structure. Since the state B only had a slightly higher value than the state D, it indicated that PU-rich phase as the shell and PMMA-rich as the core, was preferred than the other states.

For BD/BPO systems with NCO/OH ratio = 1.0, the free energy changes were shown in Figure 9; the order of free energy change, A–C > E > B > D, was similar to the result shown in Figure 8. The preferred morphology was still

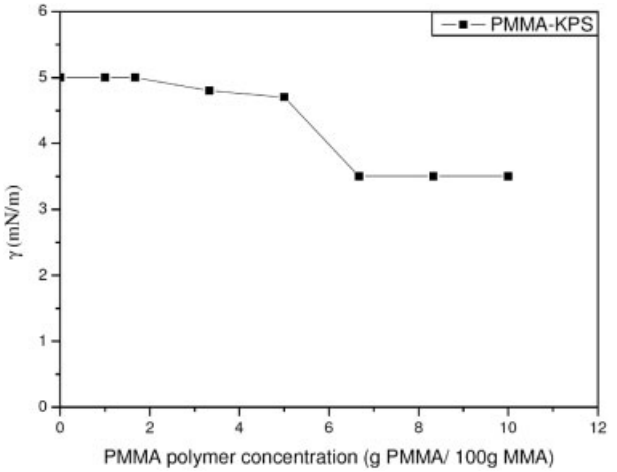

Figure 7. Interfacial tensions between PMMA-KPS/MMA and water with different PMMA polymer concentrations for PMMA-KPS system.

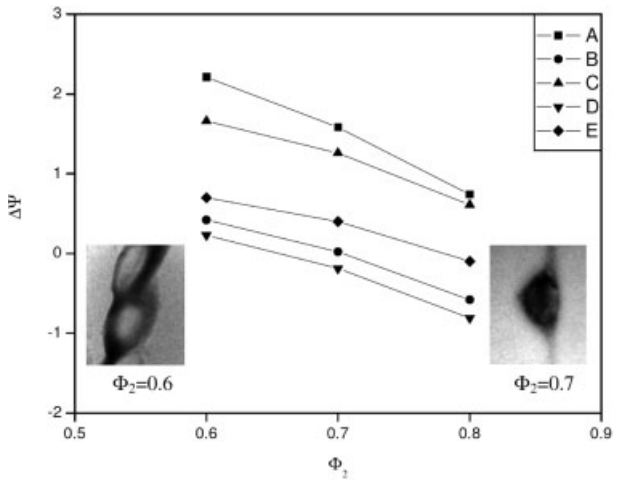

Figure 8. The predicted free energy changes of five final states for BD/BPO systems with NCO/OH = 1.7 and different volume fractions of PMMA. For case D, $\gamma_{23} = \gamma_{13} = \gamma_{12}/2$, $R_2 = 10$, $R_0 = Z$-average diameter, $\Phi_{31} = \Phi_{32} = 0.5$ for consideration.

PU-rich phase as the shell and PMMA-rich as the core.

As shown in Figure 10, the order of free energy change was A > C > E > B > D. Using water-soluble KPS initiator, it led to less difference of free energy change among the five states comparing to the system with BPO initiator. Due to using KPS initiator, PMMA chain end would have more hydrophilic ions. Then the compatibility between PU and PMMA increased. From the calculation, the preferred structure

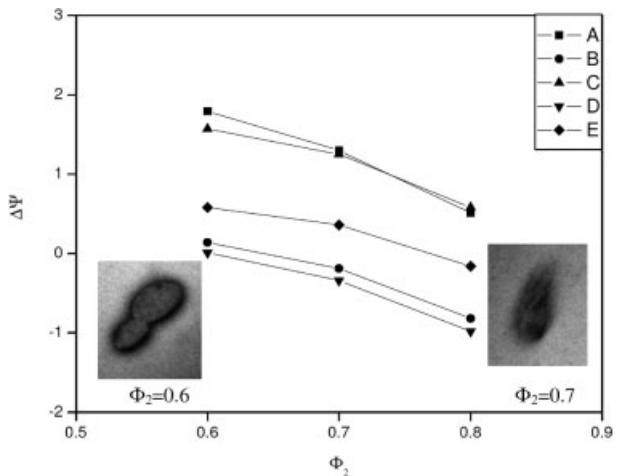

Figure 9. The predicted free energy changes of five final states for BD/BPO systems with NCO/OH = 1.0 and different volume fractions of PMMA. For case D, $\gamma_{23} = \gamma_{13} = \gamma_{12}/2$, $R_2 = 10$, $R_0 = Z$-average diameter, $\Phi_{31} = \Phi_{32} = 0.5$ for consideration.

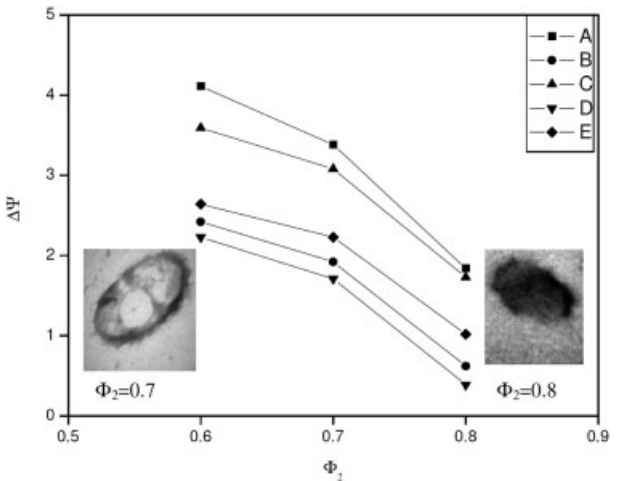

Figure 10. The predicted free energy changes of five final states for BD/KPS systems with NCO/OH = 1.0 and different volume fractions of PMMA. γ_{2W} = 4.8 based on low conversion of MMA. For case D, $\gamma_{23} = \gamma_{13} = \gamma_{12}/2$, $R_2 = 10$, $R_0 = Z$-average diameter, $\Phi_{31} = \Phi_{32} = 0.5$ for consideration.

was still PU-rich as the shell and PMMA-rich as the core.

In Figure 11, when incorporating bisphenol A as the chain extender, the difference of free energy changes among five states became smaller. It meant that using hydrophobic chain extender for PU would cause a better mixing of PU and PMMA phases. Hence, unlike previous systems, the state E showed the lowest free energy change, where the homogeneous structure was preferred. By comparing the interfacial tensions of γ_{1w} and γ_{2w}, PMMA/water had a higher interfacial tension than PU/water with BD chain extender. According to earlier papers,[9,10] polymer/water with higher interfacial tension was formed preferentially at the core of hybrid particle. Hence, the PU with BD chain extender formed core-shell particles. While in the case of using BisA as chain extender of PU, the difference of γ_{1w} and γ_{2w} became quite small, thus the homogeneous morphology of hybrid particles was possibly formed.

According to above analyses, the influences of different NCO/OH ratios and initiators of MMA on the morphology of PU/PMMA hybrid particle were not obvious. Systems of BD/BPO/1.7, BD/BPO/1.0, and BD/KPS/1.0 showed PU-rich phase as the core and PMMA-rich as the shell. However, more hydrophobic chain extender in PU phase would affect largely the morphology of hybrid particles (BisA/KPS/1.0), and showed a homogeneous structure in hybrid particles.

Comparison of TEM Observation and the Predicted Morphology from Thermodynamic Consideration

BD/BPO/1.7 System

According to TEM cross section observation, the particle of PU/PMMA = 30/70 had a core-shell structure and it was more obvious for PU/PMMA = 40/60. From thermodynamic consideration, as shown in Figure 8, the preferred final state was also a core-shell structure. The initial monomer droplet before polymerization was considered as a homogeneous phase. When a larger amount of MMA was used, the rate of polymerization of MMA became faster. Although the thermodynamically preferred state was core-shell, the core-shell structure was not very obviously observed in PU/PMMA = 30/70 because of the rapid polymerization of MMA and the morphology of hybrid particles was quickly frozen during polymerization. It meant that the kinetic effect limited the approaching of thermodynamic equilibrium. When a less amount of MMA was used, the rate of polymerization of MMA turned into slower. Hence, the particle had a more obvious core-shell structure due to the slower rate of polymerization as seen in PU/PMMA = 40/60.

BD/BPO/1.0 System

From TEM observation, PU/PMMA = 30/70 had a core-shell structure and it was more obvious for PU/PMMA = 40/60. The preferred morphology from the calculation was still core-shell. As

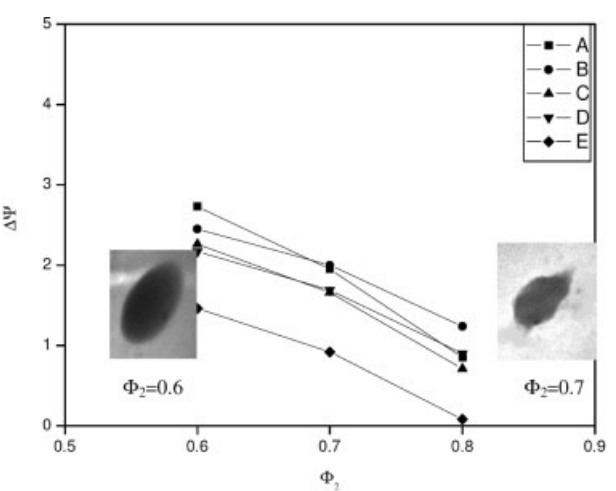

Figure 11. The predicted free energy changes of five final states for BisA/KPS systems with NCO/OH = 1.0 and different volume fractions of PMMA. For case D, $\gamma_{23} = \gamma_{13} = \gamma_{12}/2$, $R_2 = 10$, $R_0 = Z$-average diameter, $\Phi_{31} = \Phi_{32} = 0.5$ for consideration.

explained above, PU/PMMA = 30/70 system had the faster rate of polymerization and the kinetic effect led to a less core–shell morphology. However, PU/PMMA = 40/60 had the slower rate of polymerization and resulted in a more obvious core-shell structure as predicted from thermodynamic consideration.

BD/KPS/1.0 System

The morphologies of TEM observation showed that PU/PMMA = 20/80 was less of core-shell whereas PU/PMMA = 30/70 was clear in core-shell. From thermodynamic consideration, the preferred state was a core-shell structure. The reason for different morphologies of TEM observation was the same as discussed before. PU/PMMA = 20/80 had a faster rate of polymerization, hence, the kinetic effect caused less core-shell structure. On the contrary, PU/PMMA = 30/70 showed a more obvious core-shell structure due to its slower polymerization.

BisA/KPS/1.0 System

From TEM observation, both PU/PMMA = 30/70 and 40/60 of BisA/KPS/1.0 showed homogeneous structure. And the preferred morphology from the thermodynamic calculation was also homogeneous. Unlike the previous three systems, BisA/KPS/1.0 preferred the homogeneous structure and the kinetic effect was not important, because the initial state was homogeneous.

CONCLUSIONS

Based on the interfacial tensions, the free energy changes of five final states of hybrid particles with different PU/PMMA weight ratios can be calculated by thermodynamic consideration. The preferred morphology of PU/PMMA hybrid particle had the minimum free energy change. BD/BPO systems with different NCO/OH ratio showed that the minimum free energy change was state D, which was a three layer structure, that is, PU phase as the shell, PMMA phase as the core, and an intermediate layer of PU/PMMA. Using KPS initiator instead, PMMA chain end would have more hydrophilic ions. The preferred structure was still PU-rich as the shell and PMMA-rich as the core. When incorporating bisphenol A as the chain extender of PU, the free energy changes of five states became closer. It meant that using hydrophobic chain extender would cause a better mixing of PU and PMMA phases. Hence, unlike other systems, the state E showed the lowest free energy change, where the homogeneous structure of hybrid particles was preferred for system BisA/KPS/1.0.

REFERENCES AND NOTES

1. Frisch, K. C.; Klempener, D.; Migdal, S. Polym Eng Sci 1974, 15, 76–78.
2. Mohammed, S.; Daniels, E. S.; Sperling, L. H.; Klein, A.; El-Aasser, M. S. J Appl Polym Sci 1997, 66, 1869–1884.
3. Mishra, V.; Prez Du, F. E.; Gosen, E.; Goethals, E. J.; Sperling, L. H. J Appl Polym Sci 1995, 58, 331–346.
4. Wang, C.; Chu, F.; Graillat, C.; Guyot, A.; Guyot, C. Polym Adv Technol 2005, 16, 139–145.
5. Okubo, M.; Katsuta, Y.; Matsumoto, T. J Polym Sci Polym Chem Ed 1980, 18, 481–486.
6. Li, M.; Daniels, E. S.; Dimonie, V.; Sudol, E. D.; El-Aasser, M. S. Macromolecules 2005, 38, 4183–4192.
7. Wang, C.; Chu, F.; Graillat, C.; Guyot, A.; Gauthier, C.; Chapel, J. P. Polymer 2005, 46, 1113–1124.
8. Gooch, J. W.; Dong, H.; Schork, F. J. J Appl Polym Sci 2000, 76, 105–114.
9. Chen, Y. C.; Dimonie, V.; El-Aasser, M. S. J Appl Polym Sci 1991, 42, 1049–1063.
10. Chen, Y. C.; Dimonie, V.; El-Aasser, M. S. J Appl Polym Sci 1992, 45, 487–499.
11. Okubo, M.; Yamada, A.; Matsumoto, T. J Polym Sci Polym Chem Ed 1980, 16, 3219–3228.
12. Okubo, M.; Katsuta, Y.; Matsumoto, T. J Polym Sci Polym Chem Ed 1982, 20, 45–51.
13. Torza, S.; Mason, S. J Colloid Interface Sci 1970, 33, 67–76.
14. Dimonie, V. L.; El-Aasser, M. S.; Vanderhoff, J. W. Polym Mater Sci Eng 1988, 58, 821–832.
15. Chen, Y. C.; Dimonie, V.; El-Aasser, M. S. Macromolecules 1991, 24, 3779–3787.
16. Sundberg, D. D.; Casassa, A. P.; Pantazopoulos, A. P.; Muscato, M. R. J Appl Polym Sci 1990, 41, 1425–1442.
17. Kwok, D. Y.; Neumann, A. W. Can J Chem Eng 1996, 74, 551–553.
18. Lando, J. L.; Oakley, H. T. J Colloid Interface Sci 1967, 25, 526–530.
19. Potschke, P.; Pionteck, J.; Stutz, H. Polymer 2002, 43, 6965–6972.
20. Venugopal, G.; Krause, S. Macromolecules 1992, 25, 4626–4634.
21. Guschl, P. C.; Otaigbe, J. U. J Colloid Interface Sci 2003, 266, 82–92.
22. Rusanov, A. I.; Prokhorov, V. A. Interfacial Tensiometry; Elsevier: Amsterdam, 1996.
23. Wu, S. Polymer Interface and Adhesion; Marcel Dekker Inc.: New York, 1982.